Iranian Journal of Analytical Chemistry
Volume 11, Issue 2, September 2024 (40-52) Original Research Article

مجله ایرانی شیمی تجزیه
دوره ۱۱، شماره ۲، مهرماه ۱۴۰۳ (۴۰-۵۲)

Removal of Heavy Metal Ions From Polluted Water by Copper Oxide Nano-Sorbent

Hassan Karami[1,*], Anahita Ghasemi[2]
[1]Department of Chemistry, Payame Noor University, P.O. Box 19395-3697, Tehran, Iran
[2]Nano Research Laboratory, Department of Chemistry, Payame Noor University, Abhar, Iran

Received: 3 July 2024 **Accepted:** 4 September 2024
DOI: 10.30473/IJAC.2025.72395.1308

Abstract
In this work, copper oxide nano sorbent (CONS) with an average diameter of 30 nm is synthesized by polyvinyl alcohol-based sol-gel method to remove heavy metal ions from an aqueous solution. The produced nanopowder is fully characterized by transmission electron microscopy (TEM), scanning electron microscopy (SEM), X-ray diffraction (XRD), and dynamic light scattering (DLS). Various physicochemical parameters such as solution pH, nano-sorbent dosage, solution temperature, contact (mixing) time, initial concentration of lead ion, and the initial volume of lead ion sample are investigated and optimized by the "one at a time" method. Based on the experimental data, the optimum conditions for the full removal of lead ions with an initial concentration of 30 ppm, include pH 6, a sorbent dosage of 1.6 mg ml^{-1}, a solution temperature of 25 ºC, and a contact time of 13 min. The experimental results showed that the adsorption of lead ions by copper oxide nanoparticles has a good fit with Langmuir isotherm and follows the pseudo-second-order kinetics model. The experimental data shows the synthesized CuO nanoparticles are an effective sorbent for the removal of Pb(II), Fe(II), and Cu(II) from water with maximum capacities of 33.7, 20.2, and 18.8 mg g^{-1}, respectively.

Keywords
Adsorption; Characterization; Copper Oxide Nanosorbent; Heavy Metal Ion; Sol-Gel; Pollutted Water.

1. INTRODUCTION

Water pollution caused by heavy metal ions has become a serious environmental problem, especially due to their toxicity and tendency to bioaccumulate [1]. Lead is a common toxic heavy metal and it is polluted by some industries and mineral resources also lead comes from burning leaded gasoline is one of the major sources of lead entry into the atmosphere, water, and soil. Lime-stone lead can lead to waterlogging of natural origin [2]. In higher doses, they can detrimentally affect the health of most living organisms [3]. Various techniques of oxidation-reduction, coagulation, ion exchange, re-verse osmosis, and adsorption methods have been de-veloped for the removal of heavy metal ions from wa-ter [4-6]. Recent research has shown that nanostruc-tured materials as adsorbents afforded remarkable ad-vantages in the environmental application for water decontamination, owing to their large surface areas, high available surface adsorption site density, special functionality, and well-defined morphology. Compared with traditional materials and their bulk counterparts, nanostructured materials usually have advantages in environmental applications for water decontamination such as exhibiting much higher adsorption capacity and faster rates for pollutant removal [7]. Many types of sorbents, including activated carbon, oxide minerals, polymer fibers, resins, low-cost materials, and bio-sorbents, have been used to adsorb or remove Pb(II) ions from various aqueous solutions [8-13]. Particularly at the nanoscale, metal oxides are one of the precondi-tions for the recent developments in decontamination of water. Recently, the application of nanoparticles for the removal of pollutants has come up as an interesting area of research [14]. Nanoparticles exhibit good adsorption efficiency, especially due to higher surface area and greater active sites for interaction with metallic species.

Furthermore, adsorbents with specific functional groups have been developed to improve the adsorption capacity [15]. Metal oxide nanoparticles such as CuO [14], NiO [16], TiO_2 [17], and Fe_3O_4 [18] are the most commonly used materials that have been applied as adsorbents. Among metal oxides, Recently, CONS have been extensively studied as a suitable absorbent, for the removal of heavy metals because of their sim-plicity, high efficiency, and its high-speed operation in adsorption of heavy cations from aqueous solutions. One reason could be because of the interesting proper-ties of copper oxide as a p-type semiconductor with low bandwidth (1.2 eV), high-temperature superconductor alone, and doped with high magnetic resistance metals [19]. Copper oxide nanoparticles have been applied to the removal of arsenic [20], acid blue 129 [21], Hg (II) [22], ethidium bromide and ethidium mono azide [23], Cd (II), Cu (II), Ni (II), and Pb (II) [24]. In

* Corresponding author:

H. Karami; E-mail: Karami_h@pnu.ac.ir; karami_h@yahoo.com

this work, we used the poly vinyl alcohol (PVA) -based sol-gel method to synthesize copper oxide nano sorbent (CONS) for the fullest study of the removal of heavy metal ions from water.

2. EXPERIMENTAL

2.1. Materials

HNO_3, $Cu(NO_3)_2.3H_2O$, $CuSO_4.5H_2O$, $Zn(NO3)2.6H^2O$, $Fe^2(SO^4)^3.7H^2O$, $Mn(NO^3)^2.4H^2O$, $MgSO^4$, $Pb(NO^3)^2$, $NaNO^3$ and PVA (Kvalue= 72000) were purchased from Merck and used without any puri-fication. Double-distilled water was used in all experi-ments.

2.2. Instruments

The morphology and the particle sizes of the CuO sam-ple were studied by scanning electron microscopy (SEM: VEGA TS 5136M model). A transmission elec-tron microscope (TEM, Zeiss EM900, 80 keV) was used to measure the size and shape of particles accurate-ly. The dynamic light scattering (DLS) manufactured by Malvern Zetasizer (Nano ZS3600) was used to iden-tify the size distribution range. XRD spectroscopy (Philips Xpert model) was used for phase analysis of the sample. Fourier transform infrared spectroscopy (FT-IR) was used to confirm the chemical mechanism of lead ion interaction with copper oxide nanoparticles (FT-IR: Thermo Scientific, Nicolet IS10 model). A flame Atomic Absorption spectrometer (FAAS; Sens AA model, GBC Co.) was applied for the determina-tion of residual concentrations of metal ions. The pH values were controlled with a pH meter (Metrohm-827). A circulating device (PE 26 1NF model, Grant Co., England) was used to adjust the solution tempera-ture. The centrifuge (K240 model, Wagtech Co.) and cellulose acetate membranes (0.45 µ, 47 mm, Empore Co.) were used to separate the nanoparticle from the solution in adsorption and desorption experiments, re-spectively. The vacuum pump (DV-42N-2501, Plati-num Co., USA) was used to flow the solution through the membrane in the separation of CONS from heavy metal ion solutions.

2.3. Synthesis procedure

Copper oxide nanoparticles are prepared by pol-yvinyl alcohol-based sol-gel method [25]. First, 5 g Cu(NO3)2 was dissolved in 94.5 g water-ethanol (50:50) mixed solution while the stirring speed was 550 rpm. After the complete dissolu-tion of salt, 0.5 g PVA was added gradually while the solution was mixed with a stirring speed of 550 rpm and heated up to 70˚C to form a dark blue sol. After obtaining a homogeneous sol, the temperature was raised slowly (not more than 90˚C) to evaporate the solvent and form a stiff gel. With the loss of solvent and pores in the gel network, copper salt molecules are trapped in the pores. The final gel was pyrolyzed in an elec-trical furnace temperature of 500 ˚C for 2 h. During the pyrrolysis of PVA gel, copper salt is also calcined to copper oxide nanoparticles.

2.4. Adsorption experiments Cation selection

Before optimization of adsorption experiments, Fe2+, Pb2+, Zn2+, Mg2+, Mn2+, and Cu2+ solutions with the same concentration and same pH (20 ppm, pH 4) were separately mixed with 100 mg CONS for 30 min at room temperature. In all experiments, the pH adjust-ments were done by adding HNO3 or KOH. The mix-tures were centrifuged at 2500 rpm and the residual concentration of heavy metal ions was determined by FAAS. These experiments can determine which heavy metal ions can be removed from water by CONS.

2.5. Adsorption isotherm studies

Adsorption isotherms were obtained for Pb2+, Fe2+, and Cu2+ ions at three different temperatures (25, 35, and 45 ºC). For this purpose, for Pb2+ ion, five solu-tions with initial concentrations of 40, 50, 80, 100, and 150 ppm, for Fe2+, six solutions with concentrations of 20, 30, 50, 80, 100, and 150 ppm and about Cu2+, 20, 30, 50, 80, 100 and 130 ppm were prepared. pH of all solutions was 6. Each sample was mixed with 100 mg CONS and the other experimental steps were conducted according to section 2.4. Based on the residual concen-trations (Ce), the parameters of Langmuir, Freundlich, and Temkin were calculated and all isotherms were drawn.

2.6. Effect of sample dilution

To evaluate the effect of sample dilution on the remov-al efficiency, the adsorption efficiencies of CONS for lead ions for different consecutive dilutions were meas-ured. In practice, seven 50 ml lead ion solutions with pH 6 and an initial concentration of 20 ppm were pre-pared (samples 1 to 7). Different volumes of 0, 50, 100, 150, 200, 250, and 300 ml blank solution (pH= 6) were added to the samples 1 to 7 to reach the final vol-umes of 50, 100, 150, 200, 250, 300 and 350 ml, re-spectively. The adsorption experiments were performed on all the samples in the previous sections.

3. RESULTS AND DISCUSSION

3.1. Characterization of the prepared CONS

The morphology, particle size, and phase composition of the synthesized CONS were

characterized by SEM, TEM, DLS, and XRD. Fig. 1 shows the SEM and TEM images of the synthesized CONS.

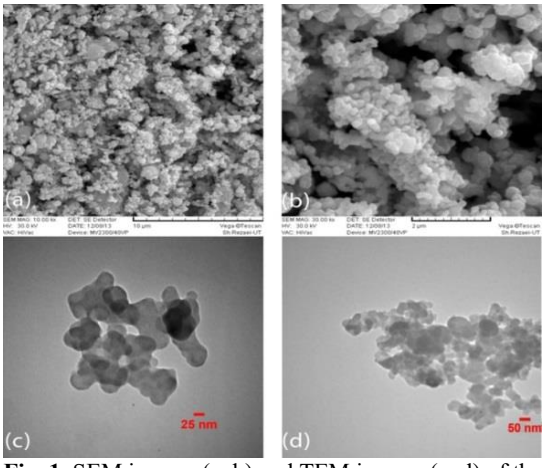

Fig. 1. SEM images (a, b) and TEM images (c, d) of the synthesized copper oxide nanoparticles.

The microstructure measurement software was used to estimate the particle size on SEM and TEM images. As is seen in Fig. 1, the sample consists of uniform nanoparticles with an average diameter of 30 nm. For more clarification about the particle size of the sample, the synthesized CONS were analyzed by DLS (Fig. 2).

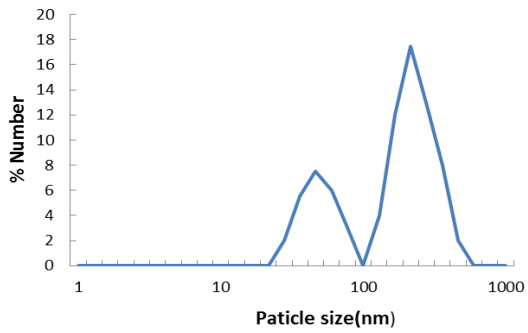

Fig. 2. Size distribution of the synthesized copper oxide nanoparticles.

As the DLS diagram shows, there are two size distribution ranges. The first distribution in the range of 50 to 100 nm is related to isolated nanoparticles and the second in the range of 150 to 600 nm is due to agglomeration of the nanoparticles.

X-ray diffraction spectroscopy is a powerful technique for phase analysis of inorganic crystalline compounds. Therefore, XRD was used for the determination of the composition of the synthesized CONS (Fig. 3). The XRD patterns were matched with those of single-phase monoclinic CuO with broad peaks at 2θ = 32.5º, 35.5º, 38.7º, 48.7º, 53.54º and 58.4º which were matched with JCPDS file number 801268. XRD patterns in Fig.3 show the synthesized sample consists only of copper oxide and there is not any impurity in the sample. Debye-Scherrer equation (D = Kλ/βcosθ) is commonly used for the calculation of the average particle size of the crystalline materials based on the base pattern (the biggest peak) in XRD patterns. By using this method, the average size of the CONS particles is calculated at 40 nm based on the peak in 2θ = 38.55 º.

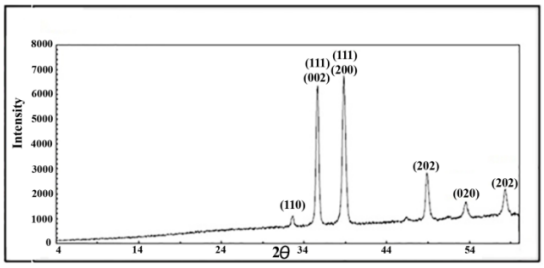

Fig. 3. XRD patterns of the copper oxide nanopowder.

3.2. Cation selection

The synthesized CONS were used for the removal of some heavy metal ions from water. The removal efficiencies were calculated by the following equation (Eq. 1):

$$\text{Removal efficiency (\%)} = \frac{C_i - C_f}{C_i} \times 100 \qquad (1)$$

Where, C_i and C_f are the initial and the residual concentrations of heavy metal ion (mg L^{-1}) before and after contact with CONS, respectively. The obtained efficiencies for the investigated ions are shown in Fig. 4. Based on the presented results, lead ions can be quantitatively removed from the polluted water (Removal efficiency was more than 95%). Iron and zinc ions also can be removed from water with efficiencies of about 62%.

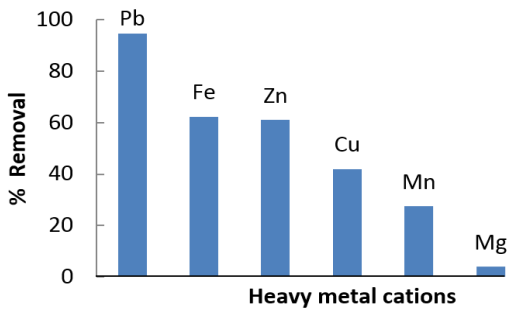

Fig. 4. Removal efficiencies of some heavy metal ions on CONS.

3.3. Adsorption mechanism

FT-IR analysis was performed to characterize the surface nature of the resulting CuO nanoparticles (Fig. 5).

The presence of a band at 590.85 cm^{-1} before lead ion adsorption (Fig. 5a) is due to the stretching vibration of the Cu–O bond. After lead ion adsorption, because of bond formation between lead and oxygen on CONS (Pb–O), the Cu–O vibration bands at 590.85 and 1384.01 cm^{-1} (Fig. 5a) are shifted to 593.90 and 1363.01 cm^{-1} (Fig.

DOI: 10.30473/IJAC.2025.72395.1308

5b). After lead ion adsorption, the presence of new bands at 712.81 and 873.40 cm^{-1} indicates different modes of bending vibration of the M–O–M (M = Pb) [26]. The vibration band at 1799.45 cm^{-1} (M-O rocks out of plane) indicates the formation of the Pb-O bond [27] or may be due to the bending vibrations of H-O-H. In Fig. 5b, the vibration band at 2514 cm^{-1} indicates the presence of the symmetric stretching vibration of the O-H bond or indicates the interaction of lead ions with the hydroxyl functional group.

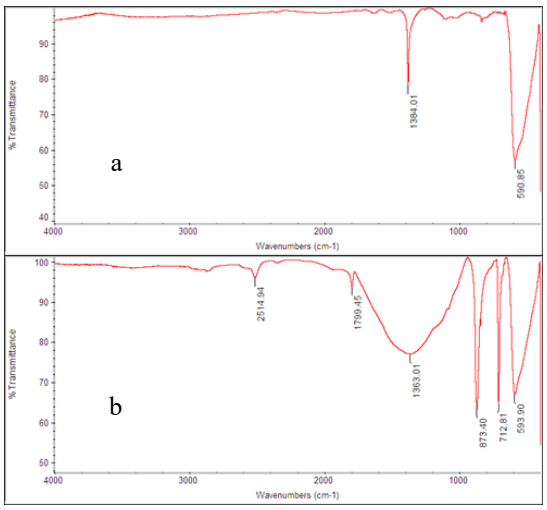

Fig. 5. FT-IR spectrums of CuO nanoparticles:(a) before and (b) after contact with lead ion solutions.

3.4. Adsorption kinetics

Adsorption kinetics studies of Pb^{2+}, Fe^{2+}, and Cu^{2+} on the CuO nanoparticles were carried out as a function of contact time. The kinetics of Pb^{2+}, Fe^{2+}, and Cu^{2+} adsorption on CuO nanoparticles were obtained by batch studies for initial concentrations of 20 mg L^{-1}, 40 mg $^{-1}$, and 60 mg L^{-1} at pH 6.0. In all of these experiments, 100 mg adsorbent was mixed with 50 ml of each metal ion solution. To investigate the time dependency of ion removal, the removal of lead ions was determined at different contact times of 2, 7, 9, 13, 20, 25, 35, 60, 75, and 255 min. Fig. 6 shows the time dependency of lead ion sorption on CONS.

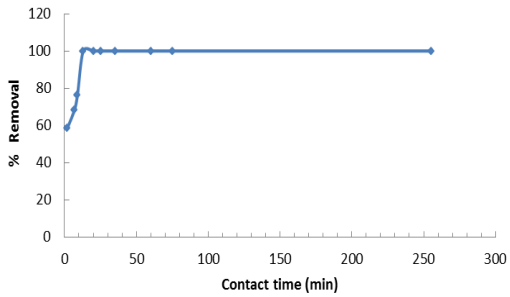

Fig. 6. Effect of contact time on the sorption of Pb^{2+} on CONS.

The lead ion removal increases from 60 to 100% during contact time of 2 to 13. The results indicate the fast sorption of lead ions on CONS. The contact time of 13 min is much shorter than those of the previous reports such as Table 1. In the following, the adsorption data was fitted to pseudo-first-order kinetic model, which is given by Eq. (3). The equilibrium adsorption capacity, q_e(mg g^{-1}) of heavy metal ions was calculated using the mass balance equation (Eq. 2):

$$q_e = \frac{(C_i - C_e)V}{m} \quad (2)$$

Where, V (ml) is the sample volume, and m (mg) is the mass of the CuO nanoasorbent.

$$\log(q_e - q_t) = log q_e - \frac{k_1}{2.303}t \quad (3)$$

Where q_e and q_t are the amounts of adsorbed ions (mg g^{-1}) at equilibrium time and at contact times t (min), respectively. K_1 is the pseudo-first-order rate constant (min^{-1}). Second, the pseudo-second-order kinetic model was studied (Eq. 4):

$$\frac{t}{q_t} = \frac{1}{k_2 q_e^2} + \frac{t}{q_e} \quad (4)$$

Table 1. Comparison of contact time of some CuO nanostructures for adsorption Pb(II) from aqueous solution.

Adsorbents	contact time(min)	Ref.
CuO nanoparticle-modified activated carbon	25	[21]
CuO nanoparticles	30	[20]
CuO nanorods	90	[28]
CuO nanostructures	240	[14]
CuO nanoparticles	300	[29]
CuO nanoparticles	13	This study

The rate constant k_2 can be obtained from the intercept of the linearized pseudo-second-order rate equation. If the pseudo-second-order equation can fit the adsorption data, there should be good linearity between t/q_t and t. The pseudo-second order equation assumes that the adsorption process involves a chemisorption mechanism and the rate of site occupation is proportional to the square of the number of unoccupied sites [30]. The pseudo-first-order and pseudo-second-order kinetics plots for the adsorption of Pb^{2+}, Fe^{2+}, and Cu^{2+} ions on CONS are shown in Fig. 7.

The presented data in Table 2 show obviously that the adsorption kinetics of the studied metal ions on CONS well fitted with the second-order kinetics plot. Therefore, it can be concluded that the adsorptions of heavy metal ions on CONS are chemisorption.

DOI: 10.30473/IJAC.2025.72395.1308

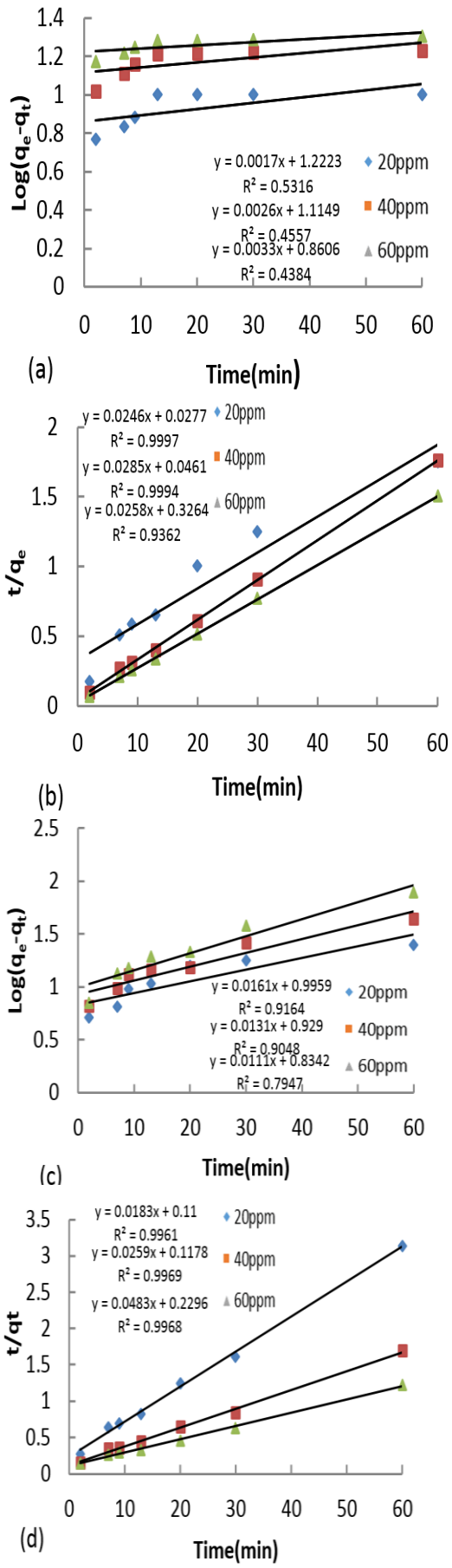

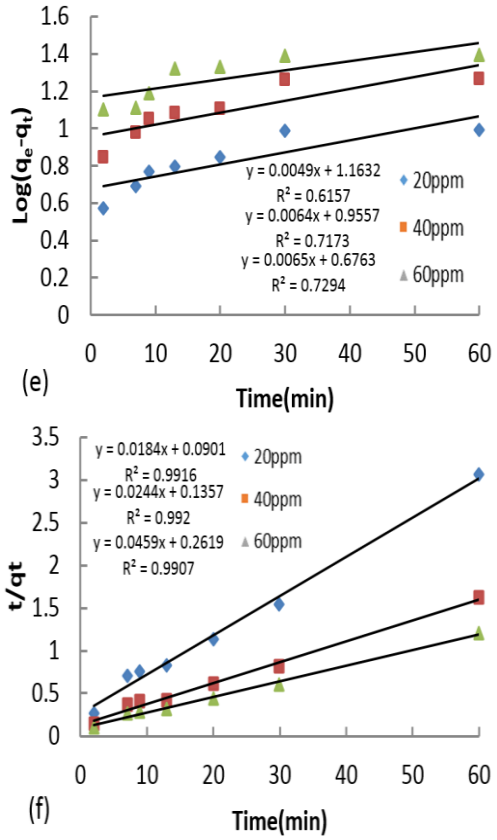

Fig. 7. Regressions of kinetic plots for CuO nanostructures: (a) pseudo-first-order model for Pb^{2+}, (b) pseudo-second- order model for Pb^{2+}, (c) pseudo-first-order model for Cu^{2+}, (d) pseudo-second-order model for Cu^{2+} , (e) pseudo-first-order model for Fe^{2+}, (f) pseudo-second-order model for Fe^{2+}.

The kinetics parameters were calculated based on the kinetics plots of Fig. 7 and summarized in Table 1.

Table 2. Kinetic parameters of the adsorption of three heavy metal ions on CONS.

Metal ions	C_0 (ppm)	First order kinetics	Second order kinetics
		K_1(min^{-1}) R^2	K_2($gmg^{-1}min^{-1}$) R^2
Pb(II)	20	1.165 0.4384	3.063 0.9362
	40	0.896 0.4557	21.691 0.9994
	60	0.818 0.5316	36.101 0.9997
Cu(II)	20	1.198 0.7947	4.355 0.9968
	40	1.076 0.9047	8.488 0.9969
	60	1.004 0.9164	9.090 0.9961
Fe(II)	20	1.478 0.7294	3.818 0.9907
	40	1.046 0.7173	7.369 0.9920
	60	0.859 0.6157	11.098 0.9916

DOI: 10.30473/IJAC.2025.72395.1308

3.5. Isothermal sorption studies

The initial concentration of the analyte is an important parameter that could affect the sorption efficiency. To evaluate this factor, seven solutions with concentrations of 20, 30, 40, 50, 80, 100, and 150 ppm lead ions were prepared by adjusting the pH at 6. The sorption process and the determination of the residual concentration of lead ions were performed according to section 2.4. Fig. 8 shows the effect of initial analyte concentration on the removal efficiency.

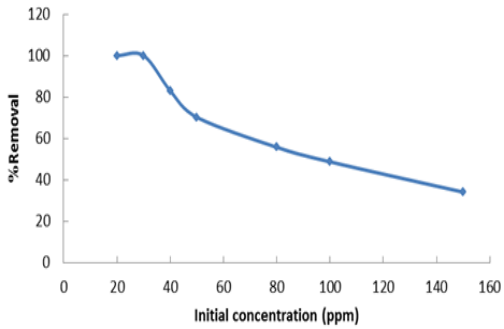

Fig. 8. Effects of initial Pb^{2+} concentration on the removal efficiency. In all of these experiments, 100 mg CONS were mixed with 50 ml lead ion solution with different initial concentrations.

As can be seen in Fig. 8, 100 mg CONS can quantitatively adsorb lead ions from 50 ml solution with an initial concentration of 30 ppm. At concentrations higher than 30 ppm, the removal amount is decreased because the adsorption sites on CuO nanoparticles are saturated. The relationship between the amount of a substance adsorbed per unit mass of adsorbents and its concentration in the equilibrium solution at constant temperature is called the adsorption isotherm. Adsorption isotherm is important to describe how solutes interact with the sorbent. Developing an appropriate isotherm model for adsorption is essential to the design and optimization of adsorption processes. Several isotherm models have been developed for evaluating the equilibrium adsorption of compounds on adsorbents, such as Langmuir, Freundlich, and Temkin [14]. Langmuir, Freundlich, and Temkin isotherm models were applied for the sorption of Pb^{2+}, Cu^{2+}, and Fe^{2+} ions on cons. In these experiments, adsorptions were carried out three at temperatures 25, 35, and 45℃ at pH 6 (Optimum pH) and over an initial concentration range from 20 to 150 ppm. In the Langmuir model, it is assumed that all the adsorption sites of the adsorbent have an identical binding energy and each site binds to only a single adsorbent [31]. The Langmuir isotherm in linear form is given as:

$$\frac{C_e}{q_e} = \frac{1}{k_L} + \frac{a_L C_e}{k_L} \quad (5)$$

Where q_e is the equilibrium adsorption capacity of adsorbent for metal ions in mg g^{-1}, C_e is the equilibrium concentration of metal ions in mg L^{-1}, K_L (L/mg), and a_L are Langmuir constants.

On the contrary, the Freundlich model is based on reversible heterogeneous adsorption; heterogeneity of binding energies of adsorption sites [31]. The linearized Freundlich isotherm can be given as follows:

$$log q_e = log k_f + \frac{1}{n} log C_e \quad (6)$$

Where K_f is the constant related to the adsorption capacity of the adsorbent in mg L^{-1}, and n is the constant related to the adsorption intensity.

The Temkin model contains a factor that clearly shows the interactions between the sorbent particles and adsorbed ions. Linearized Temkin isotherm can be presented as follows:

$$q_e = BlnA + BlnC \quad (7)$$

In this equation, $B = \frac{RT}{b}$ is the constant proportional to the heat of sorption, b is the constant in j mol^{-1} and A is the binding constant related to the maximum binding energy in L mg^{-1}. The adsorption isotherms of three metal ions on the CONS are shown in Fig. 9. All parameters of the studied isotherm models are summarized in Table 2. The presented data in Fig. 9 as well as Table 2 shows that the sorption data for Pb^{2+}, Cu^{2+}, and Fe^{2+} are better fit with the Langmuir isotherm model than the others in all temperatures.

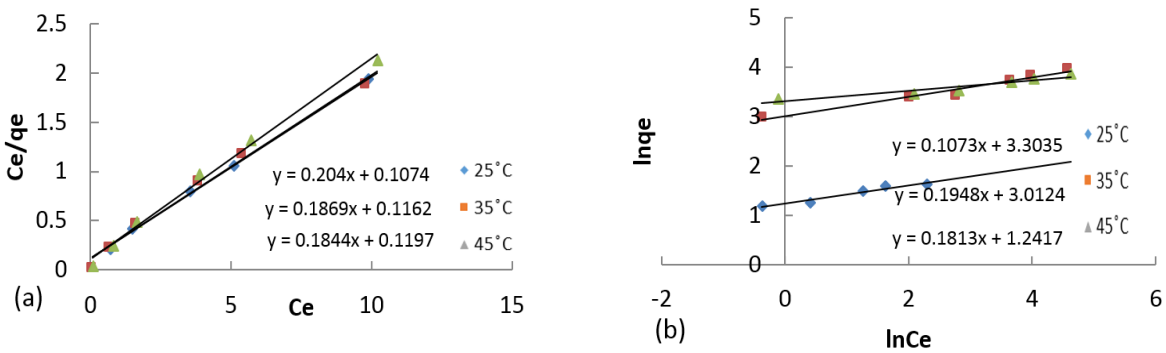

DOI: 10.30473/IJAC.2025.72395.1308

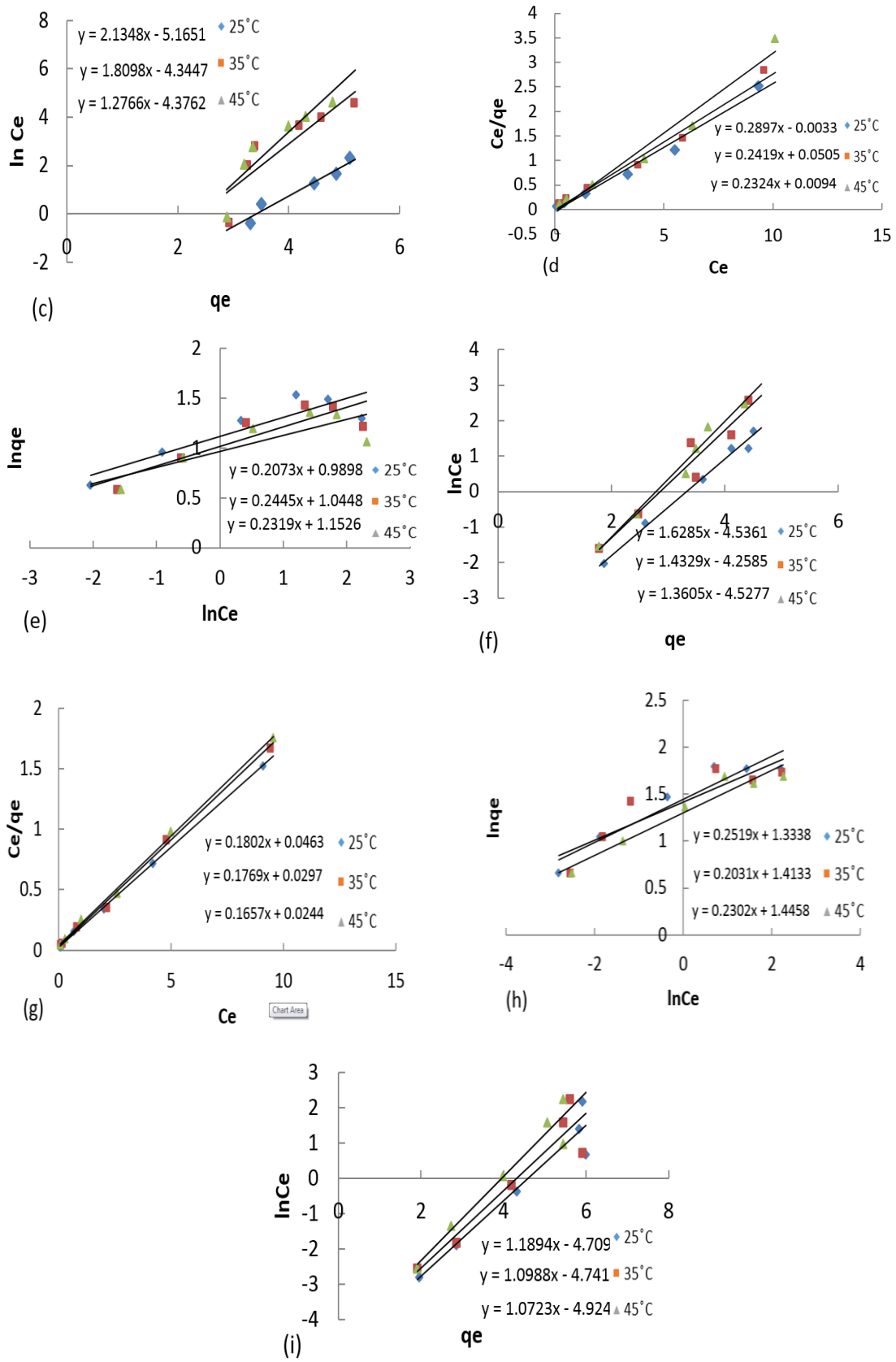

Fig. 9. Langmuir (a), Freundlich (b) and Temkin (c) isotherm models for Pb^{2+} adsorption, Langmuir (d), Freundlich (e) and Temkin (f) isotherm models for Cu^{2+} adsorption, Langmuir (g), Freundlich (h) and Temkin (i) isotherm models for Fe^{2+} adsorption.

DOI: 10.30473/IJAC.2025.72395.1308

Table 3. Isotherm parameters of metal ions sorption onto the synthesized CuO nanoparticles.

Metal	Isotherm model	Parameters	45ºC	35ºC	25ºC
Lead Ion (Pb^{2+})	Langmuir	q_{max} (mgg^{-1})	32.237	38.012	33.697
		k_l (Lmg^{-1})	9.310	8.605	8.354
		R^2	0.993	0.989	0.998
	Freundlich	K_F (mg g^{-1})(Lmg^{-1})$^{1/n}$	27.207	20.336	3.464
		n	9.319	5.133	5.515
		R^2	0.880	0.963	0.953
	Temkin	A	0.088	0.090	0.032
		B B	2.134	1.809	1.276
		R^2	0.841	0.797	0.954
Copper Ion (Cu^{2+})	Langmuir	q_{max} (mg g^{-1})	17.928	18.454	18.835
		k_l (Lmg^{-1})	303.030	19.801	106.382
		R^2	0.993	0.998	0.997
	Freundlich	K_F (mg g^{-1})(Lmg^{-1})$^{1/n}$	2.690	2.842	3.166
		n	4.823	4.089	4.312
		R^2	0.938	0.963	0.970
	Temkin	A	0.061	0.051	0.035
		B	1.628	1.432	1.360
		R^2	0.979	0.965	0.987
Iron Ion (Fe^{2+})	Langmuir	q_{max} (mg g^{-1})	20.311	19.951	20.188
		k_l (Lmg^{-1})	21.598	3.670	40.983
		R^2	0.998	0.999	0.999
	Freundlich	K_F (mg g^{-1})(Lmg^{-1})$^{1/n}$	3.795	4.109	4.245
		n	3.969	4.923	4.344
		R^2	0.972	0.799	0.913
	Temkin	A	0.019	0.013	0.010
		B B	1.189	1.098	1.072
		R^2	0.942	0.896	0.932

The maximum sorption capacities (q_{max}) of Pb^{2+}, Cu^{2+}, and Fe^{2+} ions were calculated based on the slopes of Langmuir isotherm plots. The results (Table 3) show that the heavy metal ions (Pb^{2+}, Cu^{2+}, and Fe^{2+} ions) can be adsorped with the highest capacities of 33.7, 18.8, and 20.2 mg g^{-1}, respectively.

The obtained adsorption capacity was compared with those of previous reports (Table 4). The presented data shows CONS revealed a big adsorption capacity for the removal of lead ions.

Table 4. Comparison of monolayer maximum adsorption capacities of some adsorbents for Pb (II) from aqueous solution.

Adsorbents	Maximum adsorption capacities (mg g^{-1})	References
Pb (II) -imprinted polymer	22.7	[32]
MWCNTs/iron oxide	12	[33]
ZnO Nanosheets	6.7	[34]
CeO_2 Nanocrystals	9.2	[35]
CuO nanoparticles	33.7	This study

3.6. Effect of pH

The heavy metal ions adsorption is strongly pH dependent, and so the pH of the aqueous solution is an important controlling parameter in the heavy metal ions adsorption process [36]. Among the cations used in this work, Cations Pb^{2+}, Cu^{2+}, Zn^{2+} and Fe^{2+} to a greater extent By the CONS from aqueous solutions were absorbed. So the influence of initial pH on the adsorption percentage of the cations mentioned was studied in the range of 2–7 (Fig. 10). For this purpose, solutions of 50 ml of each metal ion with initial concentrations of 20 mg $L^{-1}$was prepared. The removal efficiencies of Pb^{2+}, Cu^{2+}, Zn^{2+}, and Fe^{2+} metal ions as a function of equilibrium pH is shown in Fig. 10a. At pHs lower than 4, adsorption of metal ions is less because H^+ concentration is higher than those of metal ions. Therefore, some sorption sites of CONS are occupied by hydrogen ions and so, the metal ion adsorption is decreased. Lead ion adsorption is completed at pHs higher than 4. The zinc ion removal decreases at pHs higher than 4 because of $Zn(OH)^+$ formation. The removal of Fe^{2+} and Cu^{2+} is increased up to pH 6. Therefore, in a mixed sample, pH 6 can be used for the simultaneous removal of Pb^{2+}, Fe^{2+}, and Cu^{2+}. For further discussion on how the effect of pH on the ion removal efficiency, the point of zero charge (pH_{PZC}) of copper (II) oxide was conducted at different pH values. It was observed that the pH_{PZC} value of copper (II) oxide nanoparticles is at pH=5.8 which concluded that the sorbent surface

had a negative charge at pHs higher than 5.8 (Fig. 10b).

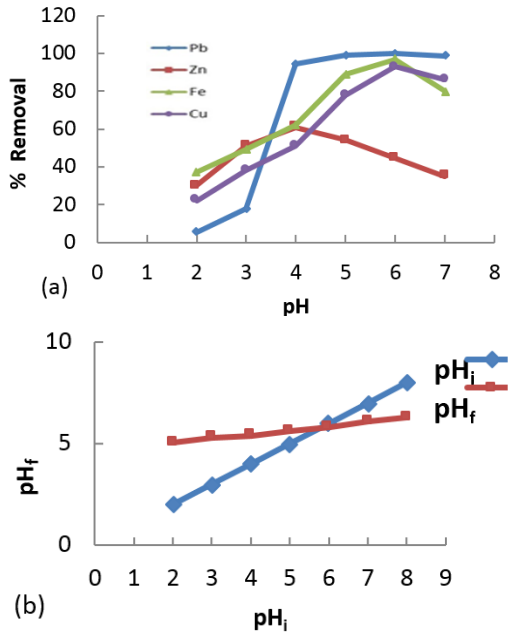

Fig. 10. Effect of pH on the sorption of Pb^{2+}, Cu^{2+}, Zn^{2+}, and Fe^{2+} ions on CONS (50 ml, 20 ppm, 30 min) (a) and the results of pH experiments to determine the point of pHpzc (b).

3.7. Effect of The adsorbent dose

The effect of CONS dosage on the removal percentage of Pb^{2+} at 7 different initial concentrations of 0.4, 0.8, 1.2, 1.6, 1.8, 2, and 2.4 mg ml^{-1} for 50 ml lead ion solutions with the same initial concentrations of 30 mg L^{-1} was shown in Fig. 11. It is obvious in Fig. 11 that the 1.6 mg ml^{-1} sorbent dosage is enough to remove quite lead ions. Using sorbent in amounts greater than 1.6 g does not affect the amount of lead ions that will be removed. A large reduction is observed in the amount of lead ion removal from 100 to 35% when the CONS dosage is decreased from 1.6 to 0.4 mg ml^{-1}. The observed removal decrease is due to the lack of adequate sites.

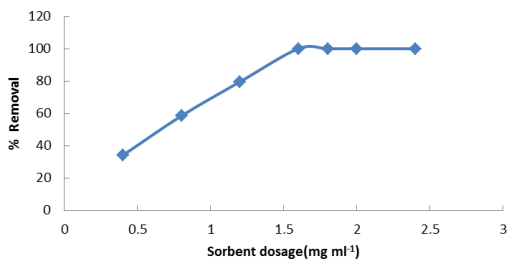

Fig. 11. Dependency of lead ion removal on the CONS dosage.

3.8. Temperature dependency of lead ion removal

To investigate the temperature dependency of ion removal, the sorption experiments of lead ions by CONS were repeated in several solution temperatures (50 ml, 20 ppm, 30 min) (Fig. 12). As Fig. 12 shows, the removal efficiency increases from 50 to 100% when the solution temperature increases from 5 to 25 ºC. In the temperature range of 5 to 25 ℃, the positive temperature dependency of lead ion removal shows endothermic sorption of lead ions. At temperatures, more than 25 ℃, the removal efficiencies are near 100% therefore, at a constant initial concentration of lead ions, the removal efficiencies are constant up to 75 ℃. The complete adsorption of lead ions up to 75°C indicates the stability of the nanosorbent surface and the stability of lead ions in solution. Adsorption study at a temperature of 80°C shows that the lead ion removal efficiency decreases. Adsorption studies at temperatures higher than 75°C have many problems, including water evaporation and rapid reduction in solution volume. Therefore, higher temperatures were not studied.

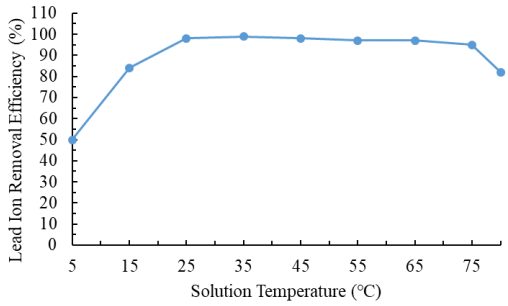

Fig. 12. Effect of solution temperature on the removal of Pb(II) ions by CONS.

3.9. Effect of sample volume

To investigate the effect of the initial volume of the sample while other parameters are kept constant, seven lead ion samples with different initial volumes in the range of 50 to 350 ml were examined (Fig. 13). In all of the samples, the absolute amount of lead ions was same (1.5 mg). Volume As illustrated in Fig13, the lead ion removal is independent from the sample volume in the range of 50 to 200 ml but, it decreases when the initial volume increases from 200 to 350 ml. The observed results of lead ion removal in the last range imply that the sorption of lead ions on CONS is an equilibrium process. For more clarification, the lead ion sorption can be shown in the following equations:

$$Pb^{2+}_{aq} + Site_{cons} \Leftrightarrow Pb^{2+}.Site_{cons} \quad (8)$$

$$K = \frac{[Pb^{2+}.Site_{cons}]}{[Pb^{2+}_{aq}][Site_{cons}]} \quad (9)$$

Where, Pb^{2+}_{aq} is lead ion in solution, $Site_{CONS}$ is the active site on CONS, $Pb^{2+}.Site_{cons}$ is the occupied site via lead ions on CONS and K is the equilibrium constant. In more diluted solutions

(initial volume bigger than 200 ml), the residual concentration (mol L^{-1}) is decreased. Therefore, to keep constant the equilibrium, much more lead ions should be free in the solution.

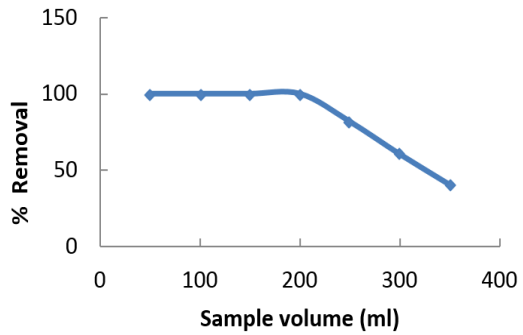

Fig. 13. Effect of initial sample volume on lead ion removal.

3.10. Application of CONS for the removal of some other heavy metal ions

For evaluation of the sorption ability of some other heavy metal ions on CONSs, many experiments were performed as Table 3. In these experiments, 300 mg CONS were added to a 50 ml mixed solution containing Pb^{2+}, Mn^{2+}, Cu^{2+}, Zn^{2+}, Mg^{2+}, and Fe^{2+} ions with initial concentrations of 30 mg L^{-1} at pH 6. The mixture was stirred and then, the residual concentrations of the mentioned ions were determined. As can be seen in Table 5, the presence of other ions can not affect the lead ion removal. On the other hand, the presented data shows that CONS not only can quantitatively remove the lead ions in the mixed solution but also can considerably adsorb the other heavy metal ions. Therefore, the synthesized CONS can act as a highly efficient sorbent for the water purification process.

Table 5. Removal efficiencies of some heavy metal ions by CONS in a mixed solution.

Cations	Pb^{2+}	Mn^{2+}	Cu^{2+}	Zn^{2+}	Mg^{2+}	Fe^{2+}
Removal (%)	98 %	85%	75 %	35 %	76%	90 %

3.11. Thermodynamic study

The effect of temperature on an adsorption process depends on its mechanism. Temperature has two major effects on these processes. The first is the direct dependency of the diffusion rate of the sorbate across the external boundary layer and in the internal pores of the adsorbents. The variation of equilibrium capacity of the sorbent towards sorbate is the second temperature effect in such processes[37-38].

To investigate the influence of temperature on the uptake of lead ions by the studied adsorbents, the removal of these ions (20 mg L^{-1}) from aqueous solution, adjusted at pH 6, by 100 mg of CONS sorbent was performed as a function of temperature in the range 278-338 K. The corresponding distribution coefficient(K_d) was calculated by(E_q. 10):

$$K_d = \frac{(C_0 - C_e)}{C_e} \times \frac{V}{m} \quad (10)$$

Where C_0 and C_e are initial and equilibrium concentrations of lead ions (mg L^{-1}), respectively, V is the volume of the aqueous phase solution (L) and m is the amount of adsorbent (g).

The Van't Hoff equation (E_q. 11):

$$lnK_d = -\frac{\Delta H^{\circ}}{RT} + \frac{\Delta S^{\circ}}{R} \quad (11)$$

Conducts calculating enthalpy (ΔH^o) and entropy changes (ΔS^o), by analysis of the lnK_d versus T^{-1} plot. The values of ΔH^o and ΔS^o were calculated from the slope and intercept of the linear plot of lnK_d versus T^{-1}, respectively [37]:

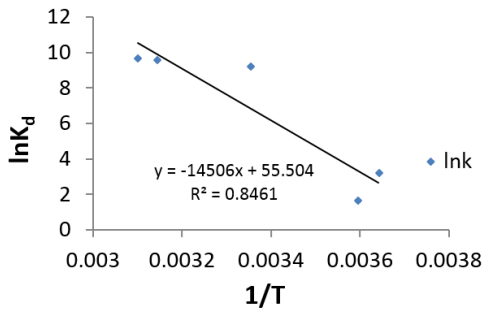

Fig. 14. Variation of equilibrium constant (K_d) as a function oftemperature (1/T).

The Gibbs free energy changes (ΔG^o), thus can be determined by (Eq. 12):

$$\Delta G^o = \Delta H^o - T\Delta S^o \quad (12)$$

The calculated thermodynamic parameters for the adsorption process of lead ions on the adsorbent are given in Table 6.

Table 6. Values of various thermodynamic parameters for adsorption of Pb(II) on Cuo adsorbent.

Adsorbent	ΔH^o(kJ mol^{-1})	ΔS^o($Jmol^{-1}K^{-1}$)		
CONS	120.602	461.460		
ΔG^o (kJ mol^{-1})				
278K	288K	298K	310K	338K
-7.683	-12.298	-16.95	-22.45	-35.419

The positive value of enthalpy changes reveals the adsorption of lead ions by CONS is controlled by entropy changes. In our study, the positive values of ΔH^o confirmed the endothermic nature of the process. The negative ΔG^o value indicated a spontaneous process.

4. CONCLUSIONS

Polyvinyl alcohol-based sol-gel pyrolysis method is a fast, environmentally friendly, and low-cost

DOI: 10.30473/IJAC.2025.72395.1308

procedure to synthesis metal oxide nanoparticles. The current research confirm that the CuO nanoparticles with average particle diameter of 30 nm can easily prepared by the introduced sol-gel method. The prepared CuO nanoparticles exhibited predominant adsorption ability to heavy metal ions which may be attributed to large specific surface areas and the existence of nanoporous structure. The lead ions can quantitatively removed from polluted waters by the presented CuO nanosorbent.

Acknowledgment
We gratefully acknowledge the support of this work by Abhar Payame Noor University Research Council.

REFERENCES

[1] A. Sari, M. Tuzen, Biosorption of cadmium(II) from aqueous solution by red algae (Ceramium virgatum): equilibrium, kinetic and thermodynamic studies, *J. Hazard. Mater*., 157 (2008) 448.
[2] C.B. Ernhart, A critical review of low-level prenatal lead exposure in the human: 1. Effects on the fetus and newborn, *Reprod. Toxicol.*, 6 (1992) 9.
[3] C. Gheorghiu, D. J. Marcogliese, Effects of waterborne zinc on reproduction, survival and morphometrics of Gyrodactylus turnbulli (Monogenea) on guppies, *Int. J. Parasitol.* 37 (2007) 375.
[4] N.A.A. Qasem, R.H. Mohammed, D.U. Lawal, Removal of heavy metal ions from wastewater: a comprehensive and critical review, *NPJ. Clean Water* 36 (2021) 1.
[5] O.B. Apea, B.E. Akorley, E.O. Oyelude, B. Ampadu, Evaluation of the adsorption behavior and divalent metal ions removal efficiency of ceramic point-of-use water filter materials, *Environ. Sys. Res*., 12 (2023) 37.
[6] M. Hosseini, M. Rezaei, Synthesis, Characterization, and Application of 1-Methyl-2-hexylthioimidazolium Chloride Liquid for Solvent-based Microextraction (SBME) of Hg in Water Samples, *Anal. Bioanal. Chem. Res.*, 11 (2024) 423.
[7] L. Ai, Y. Zeng, Hierarchical porous NiO architectures as highly recyclable adsorbents for effective removal of organic dye from aqueous solution, *Chem. Eng. J.* 215 (2013) 269.
[8] H.T. Fan, X.T. Sun, Z.G. Zhang, W.X. Li, Sb(III)-Imprinted Organic-Inorganic Hybrid Sorbent Prepared by Hydrothermal-Assisted Surface Imprinting Technique for Selective Adsorption of Sb(III), *J. Chem. Eng.* 59 (2014) 2106.
[9] F. Rostamkhani, H. Karami, A. Ghasemi, Application of nickel oxide nanoparticles as reusable sorbent for the removal of lead ions from contaminated water, Chem. Eng. J., 60 (2017) 319.
[10] D.P. Sui, H.X. Chen, L. Liu, M.X. Liu, C.C. Huang, H.T. Fan, Ion-imprinted silica adsorbent modified diffusive gradients in thin films technique: Tool for speciation analysis of free lead species, *Talanta*. 148 (2016) 285.
[11] L. Q. Vo, A.T. Vu, T.D. Le, C.D. Huynh, H.V. Tran, Fe3O4/Graphene Oxide/Chitosan Nanocomposite: A Smart Nanosorbent for Lead(II) Ion Removal from Contaminated Water, *ACS Omega,* 9 (2024) 17506.
[12] B. Viltuznik, A. Kosak, Y.L. Zub, A. Lobnik, Removal of Pb(II) ions from aqueous systems using thiol-functionalized cobalt-ferrite magnetic nanoparticles, *J. Sol Gel. Sci. Technol.* 68 (2013) 365.
[13] E.O. Ryabchenko, A.P. Suslov, N.A. Morozov, E.F. Krivoshapkina,Silica/carbon dot nanosorbent for detection and removal of Pb(II) and Co(II) ions from wastewater, *Chem. Eng. J*., 500 (2024) 156610.
[14] A.A. Farghali, M. Bahgat, A.Enaiet Allah, M.H. Khedr Adsorption of Pb(II) ions from aqueous solutions using copper oxide nanostructures, *Beni-Suef University. J. Bas. Appl. Sci.,* 35 (2013) 61.
[15] A.R. Turker, New Sorbents for Solid-Phase Extraction for Metal Enrichment, *Clean. Soil. Air. Water*. 35 (2007) 548.
[16] R. Wang, Q. Li, D. Xie, H. Xiao, H. Lu, Synthesis of NiO using pine as template and adsorption performance for Pb (II) from aqueous solution, *Appl. Surf. Sci.* 279 (2013) 129.
[17] K.E. Engates, H.J. Shipley, Adsorption of Pb, Cd, Cu, Zn, and Ni to titanium dioxide nanoparticles: effect of particle size, solid concentration, and exhaustion, *Environ. Sci. Pollution. Res.* 18 (2010) 386.
[18] H. Karami, Heavy metal removal from water by magnetite nanorods, *Chem. Eng. J.* 219 (2013) 209.
[19] D.P. Singh, N. Ali, Synthesis of TiO2 and CuO nanotubes and nanowires, *Sci. Adv. Mater*. 2 (2010) 295.
[20] C.A. Martinson, K.J. Reddy, Adsorption of arsenic (III) and arsenic (V) by cupric oxide nanoparticles, *J. Colloid Interf. Sci.* 336 (2009) 406.
[21] F. Nekouei, S. Nekouei, I. Tyagi, V.K. Gupta, Kinetic, thermodynamic and isotherm studies for acid blue 129 removal from liquids using copper oxide nanoparticle-modified activated carbon as a novel adsorbent, *J. Mol. Liq.* 201 (2015) 124.
[22] A. Fakhri, Investigation of mercury (II) adsorption from aqueous solution onto copper oxide nanoparticles: Optimization using response surface methodology, *Process.Saf. Environ. Protect*. 93 (2015) 1.

[23] A. Fakhri, Assessment of Ethidium bromide and Ethidium monoazide bromide removal from aqueous matrices by adsorption on cupric oxide nanoparticles, *Ecotoxicol. Environ. Sci.* 104 (2014) 386.
[24] S. Mahdavi, M. Jalali, A. Afkhami, Removal of heavy metals from aqueous solutions using Fe3O4, ZnO, and CuO nanoparticles, *J. Nanoparticle Res.* 14 (2012) 171.
[25] R. Gholami, R.; *MSc Thesis*, Payame Noor University, Abhar, Iran. (2014).
[26] S. Jadhav, S. Gaikwad, M. Nimse, A. Rajbhoj, Copper oxide nanoparticles: synthesis, characterization and their antibacterial activity, *J. Clust. Sci.* 22 (2011) 121.
[27] A. El Trass, H. El Shamy, I. Mehasseb, M. El Kemary, CuO nanoparticles: Synthesis, characterization, optical properties and interaction with amino acids, *App. Surf. Sci.* 258 (2012) 2997.
[28] P.K. Raul, S. Senapati, A.K. Sahoo, I.M. Umlong, R.R. Devi, A.J. Thakur, V. Veer, CuO nanorods: a potential and efficient adsorbent in water purification, *RSC Adv.* 4 (2014) 40580.
[29] A. Goswami, P.K. Raulb, M.K. Purkait, Arsenic adsorption using copper (II) oxide nanoparticles, *Chem. Eng. Res. Design* 90 (2012) 1387.
[30] J. Gong, L. Chen, G. Zeng, F. Long, J. Deng, Q. Niu, X. He, Shellac-coated iron oxide nanoparticles for removal of cadmium(II) ions from aqueous solution, *J. Environ. Sci*. 24 (2012) 1165.
[31] S. Liang, X. Guo, N. Feng, Q. Tian, Isotherms, Kinetics and Thermodynamic Studies of Adsorption of Cu^{2+} from Aqueous Solutions by Mg^{2+}/K^{+} Type Orange Peel Adsorbents, *J. Hazard. Mater*. 174 (2010) 756.
[32] C. Li, J. Gao, J. Pan, Z. Zhang, Y. Yan, Synthesis, characterization, and adsorption performance of Pb(II)-imprinted polymer in nano-TiO2 matrix, *J. Environ. Sci*. 21 (2009) 1722.
[33] J. Hu, D. Shao, C. Chen, G. Sheng, J. Li, X. Wang, M. Nagatsu, Plasma-induced grafting of cyclodextrin onto multiwall carbon nanotube/iron oxides for adsorbent application, *J. Phys. Chem. B*. 114 (2010) 6779.
[34] X.F. Ma, Y.Q. Wang, M.J. Gao, Z. Xu, G.A. Li, A novel strategy to prepare ZnO/PbS heterostructured functional nanocomposite utilizing the surface adsorption property of ZnO nanosheets, *Catal. Today*. 158 (2010) 459.
[35] C.Y. Cao, Z.M. Cui, C.Q. Chen, W.G. Song, W. Cai, Ceria hollow nanospheres produced by a template-free microwave-assisted hydrothermal method for heavy metal ion removal and catalysis, *J. Phys. Chem. C*. 114 (2010) 9865.
[36] M. Y. Pamukoglu, F. Kargi, Removal of copper (II) ions from aqueous medium by biosorption onto powdered waste sludge, *Proc. Biochem*. 41 (2006) 1047.
[37] P. Sharma, R. Tomar, Synthesis and application of an analogue of mesolite for the removal of uranium (VI), thorium (IV), and europium (III) from aqueous waste, *Micropor. Mesopor. Mat*. 116 (2008) 641.
[38] S. Wang, Y. Boyjoo, A. Choueib, Z.H. Zhu, Removal of dyes from aqueous solution using fly ash and red mud, *Water. Res*. 39 (2005) 129.

COPYRIGHTS
© 2022 by the authors. Lisensee PNU, Tehran, Iran. This article is an open access article distributed under the terms and conditions of the Creative Commons Attribution 4.0 International (CC BY4.0) (http:/creativecommons.org/licenses/by/4.0)

DOI: 10.30473/IJAC.2025.72395.1308

حذف یون‌های فلزات سنگین از آب‌های آلوده توسط نانوجاذب اکسید مس

حسن کرمی*[1]، آناهیتا قاسمی[2]
[1]بخش شیمی، دانشگاه پیام نور، تهران، ایران
[2]آزمایشگاه تحقیقاتی نانو، بخش شیمی، دانشگاه پیام نور، ابهر، ایران

* E-mail: Karami_h@pnu.ac.ir; Karami_H@yahoo.com
تاریخ دریافت: ۱۳ تیر ۱۴۰۳ **تاریخ پذیرش:** ۱۴ شهریور ۱۴۰۳

چکیده
در این کار، نانوجاذب اکسید مس (CONS) با قطر متوسط ۳۰ نانومتر به روش سل-ژل مبتنی بر پلی وینیل الکل برای حذف یون های فلزات سنگین از محلول آبی سنتز می‌شود. نانوپودر تولید شده به طور کامل با میکروسکوپ الکترونی عبوری(TEM) ، میکروسکوپ الکترونی روبشی(SEM) ، پراش پرتو ایکس (XRD) و پراکندگی نور پویا (DLS) مشخصه‌یابی می‌شود. پارامترهای فیزیکی و شیمیایی مختلف مانند pH محلول، دوز نانوجاذب، دمای محلول، زمان تماس (اختلاط)، غلظت اولیه یون سرب و حجم اولیه نمونه یون سرب به روش یک عامل در یک زمان بررسی و بهینه سازی می‌شوند. بر اساس داده های تجربی، شرایط بهینه برای حذف کامل یون‌های سرب با غلظت اولیه ۳۰ ppm، pH ۶، دوز جاذب ۱/۶ $mg\ ml^{-1}$، دمای محلول ۲۵ درجه سانتیگراد و زمان تماس ۱۳ دقیقه می‌باشد. نتایج تجربی نشان داد که جذب یون‌های سرب توسط نانوذرات اکسید مس با ایزوترم لانگمویر هماهنگی خوبی دارد و از مدل سینتیک شبه مرتبه دوم پیروی می‌کند. داده‌های تجربی نشان می‌دهد که نانوذرات CuO سنتز شده به ترتیب با حداکثر ظرفیت‌های ۲۳/۷، ۲۰/۲ و ۱۸/۸ $mg\ g^{-1}$ جاذب مؤثری برای حذف یون‌های سرب(II) ، آهن (II) و مس (II) از آب می‌باشد.

کلید واژه ها: جذب؛ مشخصه‌یابی؛ نانوجاذب اکسید مس؛ یون فلزات سنگین؛ سل-ژل؛ آب آلوده.

DOI: 10.30473/IJAC.2025.72395.1308